5. DISTRIBUTED SOLUTE TRANSPORT MODELING BASED ON THE MORPHOLOGICAL CONCEPTUALIZATION OF DRAINAGE NETWORKS

Mario A. Jiménez[1], Luis A. Camacho [2] & Jaime I. Vélez[1]

[1]Universidad Nacional de Colombia –Medellín. Medellín – Colombia

[2]Universidad de los Andes. Bogotá – Colombia

ABTRACT

In this work a distributed model for solute transport modelling is conceptually described. The model is based on the use of digital elevation models as the primary source of information, and conceptualizes the drainage network as a set of connected stream reaches, which define the fundamental unit into the modelling framework. A first processing is made to derive traditional DEM products (flow direction, flow accumulation and cumulative distances), and then the raster drainage network is segmented in reaches delimited by hydrological nodes, corresponding to stream confluences, and topographical nodes at sites having significant slope breaks. Those reaches are morphologically classified, and depending on the stream type assigned, they are first sized using hydraulic geometry relations derived for bankfull width, and then characterized in terms of their properties for transport solutes downstream. Dispersion mechanisms are characterized in terms of the ADZ model's parameters.

The model was verified in La Mosca watershed using DEM with resolutions of 10 m, 30 m and 90 m, and the segmentation procedure showed to be consistent regarding hydrological and topographical nodes definition. However, slope appeared to be the more sensitive variable to changes in DEM resolution, thus influencing the channel sizing and the assignment of dispersive properties.

According with the obtained results, (1) slope sensitivity is linked more to the averaged cell elevation and how it changes with DEM resolution, than with changes in river length estimations which is not as sensitive, (2) a segmentation of drainage networks considering slope breaks, lead to differences in solute travel time and dispersion estimations as likely expected, especially, in the upper watershed areas, (3) a multi-resolution analysis is suggested for selecting the more appropriated DEM, taking into account consistency among the different sources used as well as the computational times required for the model.

Key words: *distributed model, digital elevation model, solute transport*, *hydraulic geometry*.

5.1 INTRODUCTION

Drainage network is one of the natural systems that emerge as a result of the continuos geomorphic work of water on Earth's surface, and how it responds in accordance with downstream water and sediment accumulation and its topographic, geological and lithological characteristics. Also, it is the support of various essential processes for man and society [*Rodriguez-Iturbe et al.*, 2009] including flow accumulation and development of high gradient river corridors that favor the generation of energy or consumptive water use, transport and deposition of sediment which defines sources of agricultural or mining activities, and the assimilation of dissolved substances through dispersion mechanisms which underline the use of stream for wastewater disposals.

From the hydrology and geomorphology, different strategies have been proposed to describe drainage networks. From an aggregated point of view this strategies range from hierarchical ordering methods [*Strahler*, 1957], to schemes able to transform their topology into metrics to evaluate the hydrological watershed response [*Veitzer and Gupta*, 2001; *Rodriguez-Iturber et al.*, 1982]. However, when the spatial variability of the physical processes taking place in the drainage network becomes a relevant issue, a distributed approach provides a better representation of the system, an aspect reflected on the diversity of morphological descriptors of stream bedforms, stream patterns and floodplain corridors [*Schumm*, 1985; in *Knighton*, 1998; *Leopold and Maddock*, 1953; *Montgomery and Buffington*, 1997; *Dodov and Foufoula-Georgiou*, 2005], whose assessment can be made using geospatial information.

Specifically, digital elevation models (DEMs) have become one of the main inputs to both represent the topology of drainage networks and to characterize their geometry and morphology.

Among others, this characterization includes channels sizing through downstream hydraulic geometry relations given the control exerted by geometry in flow propagation, sediment and solute transport, and the possibilities of using the drainage area as a surrogate variable of the discharge [*Burns*, 1998; *Orlandini and Rosso*, 1998; *Neal et al.*, 2012]. However, a stream hydraulic geometry is influenced, among others, by sediment supply, the degree of lateral confinement and bank resistance, which have led to propose differentiated hydraulic geometry relations in terms of quasi-universal morphological classes [*Parker et al.*, 2007; *Kellerhals and Churc*, 1989].

Beyond channel sizing, the identification of morphological classes in the drainage network has proven to be useful in the analysis of sedimentological processes, differentiation of mesoscale units, to characterize solute dispersion mechanisms [*González*, 2008; *Jiménez and Wohl*; 2013] and for homologation of the scientific communication. In such direction, as an extension of the morphological classification scheme by *Montgomery and Buffington* [1998], *Flores et al.* [2006] suggested using the longitudinal slope S_0 and the specific stream power index $S_0 A^{0.4}$ as discriminatory variables to identify the morphological types *cascade*, *step-pool*, *plane bed* and *pool-riffle* throughout the drainage network. Based on the same scheme, *Thompson et al.* [2008] also included the lithology characteristics of the alluvial corridor to differentiate morphological types. Instead of stream bed forms, other schemes has been focused in channel patterns and the stream potential for lateral migration [*Leopold and Wolman*, 1960; *Beechie et al.*, 2006; *Nicoll and Hickin*, 2010].

Regardless of the classification scheme, a reach defines the unit of analysis under the hypothesis of geomorphological stability, similar to the assumptions of stationary processes in the basin scale when setting aggregated models. However, a stream reach is usually set as a segment whose length is a multiple of the stream width, or as a fixed set of successive cells when using a raster representation of the drainage network.

In this paper we propose (1) a strategy for the segmentation and the subsequently morphological characterization of drainage networks, using digital elevation models as a primary source of information, (2) the assignation of morphological features to stream reaches according with the classification scheme presented by *Flores et al.* [2006] and the hydraulic geometry relations for bankfull width proposed in Chapter 4 for the same morphological classes and, (3) to use such drainage network conceptualization to simulate solute transport using the model ADZ [Aggregated

dead zone, *Beer and Young*, 1983] and their parameterization following the contributions made by *Camacho* [2000], *González* [2008] and *Jiménez and Wohl* [2013].

For the latter purpose, it was selected La Mosca watershed, located in the department of Antioquia (Colombia), because of the availability of geospatial information with different resolutions, favoring model verification and identification of its limitations.

5.2 MODEL STRUCTURE

The *Distributed Solute Transport Model* implementation relies on the topographic representation of the region of interest through a DEM, and its pre-processing to obtain the traditional raster products shown in Figure 5-1. Obtaining these maps is simple with geographic information systems (GIS), into which it is possible to set stream burning procedures to improve a raster representation.

A DEM selection is not trivial because properties such as spatial resolution, and the interpolation method or data capturing technology, have influence on the estimation of morphometric variables such as watershed area, slope and river length [*Paz et al.*, 2008; *Wu et al.*, 2008]. The results of different studies [*Ferguson*, 1975; *Howard and Hemberger*, 1991] suggest that DEMs having resolutions of 1 to 4 times the average stream width are suitable for the estimation of stream patterns descriptors (river length, sinusoidal, amplitude, wavelength and bend radius); by contrast, when the resolution is coarser, river length is underestimated due to meander "*cutoffs*" which are digitally generated. To minimize such effect, the Distance Transforms (DT) proposed by *Butt and Maragos* [1998] where implemented, which establish the factors 0.96194 and 1.36039 for calculating orthogonal and diagonal distances from raster analysis, instead the factors 1 and $\sqrt{2}$ when using Euclidean distances.

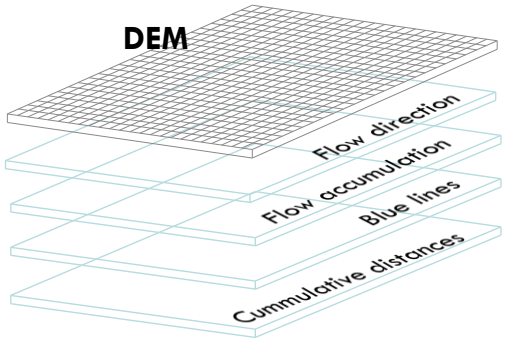

Figure 5-1. DEM pre-processing

Stream burning and DT factors define the modeling strategy here used to minimize the effect of DEM resolution on the estimation of river lengths, which have a direct influence on the estimation of travel time along the drainage network.

5.2.1 Segmentation Method

Drainage network segmentation is proposed by separating reaches delimited by two sites with hydrological and geomorphological significance. The former correspond to hydrologic nodes whose definition is made according with the identification of river confluences. The latter defines topographic nodes, which are identifying where significant downstream slope changes occur (see Figure 5-2). The longitudinal slope is one of the most significant variables to describe geomorphological units, hence that its variability was included into the segmentation strategy

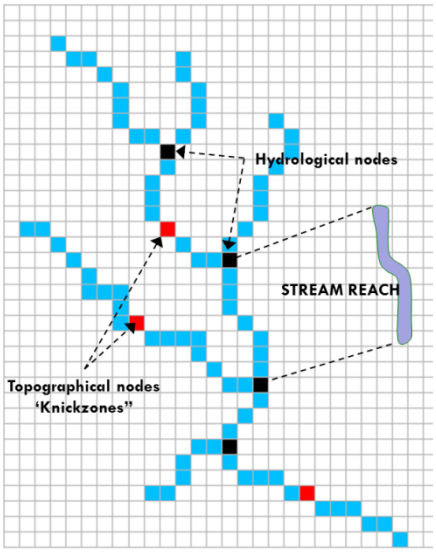

Figure 5-2. Schematic representation of nodes and reaches

For an ideal geomorphic cycle, channel slope follows a scaling relation in the form $S_0 \, \alpha \, A^{-a}$, however, forcing factors as lithology of the alluvial corridor, abrupt changes in sediment supply and/or hydrological regime and variations in lateral confinement, lead to interruptions in the geomorphic cycle shown as abrupt changes in slope. Nonetheless, regardless of the reason, DEMs provide the necessary information to identify such anomalies along a stream longitudinal profile. *Giles and Franklin* [1998] showed that topographical breaks correspond to those sites having a greater change on slope gradient δ than adjacent sites, as well as greater that a minimum threshold defined for each studied condition. However, because the method uses a searching window size of 7

cells, breakpoints could be erroneously biased by inherent errors in the construction techniques of DEMs. More recently, *Hayakawa and Oguchi* [2006] posed a method that further than local gradient, it takes into account a trend gradient and how this decreases faster at those break slope sites or *knickpoints* when increasing the window size used to calculate the slope. Consider the longitudinal profile shown in Figure 5-3, which can be extracted from a DEM. In each cell or pixel of the analyzed stream, the slope G_d can be estimated according to the expression (5-1), where z_1 y z_2 represent the elevation at cells located a distance d upstream and downstream of the cell of interest, respectively. Thereby, G_d can be considered like a centered numerical estimate. However, in this work G_d was estimated as a forward difference so that z_1 always corresponds to the elevation at the evaluated pixel. This change allowed applying the method from the beginning of the stream in its first pixel.

$$G_d = \frac{z_1 - z_2}{d} \qquad 5\text{-}1$$

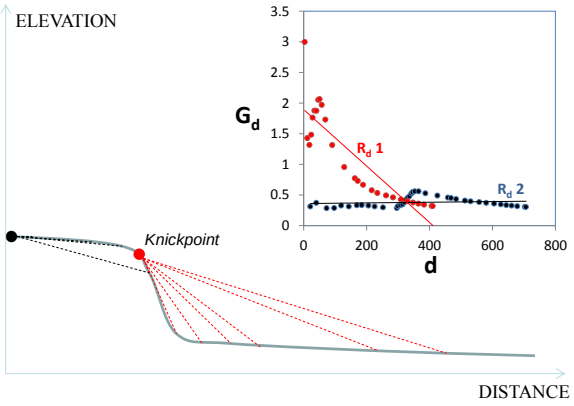

Figure 5-3. Variability of G_d with downstream distance d for two different sites (cells) along a long profile, and a higher rate change for *knickpoints* (red dots)

In those sites having an abrupt change in the slope (*knickpoints*), the diagram $G_d - d$ displays a rapid decrease with distance d, as illustrated in Figure 5-3. *Hayakawa and Oguchi* [2006] proposes estimating the metric R_d for a stream cell as the slope of the line which best fit the cloud (G_d, d). Cells with a metric lower than the standard deviation of the values R_d estimated in the whole stream, are then considered *knickpoints* or topographic nodes. Figure 5-4a illustrates the application of the method for a longitudinal profile, where red dotted lines denote the location of topographic nodes taking into account the cells having a metric R_d below the established threshold. Figure 5-4b shows the spatial location of the nodes obtained and their correspondence with the terrain topology.

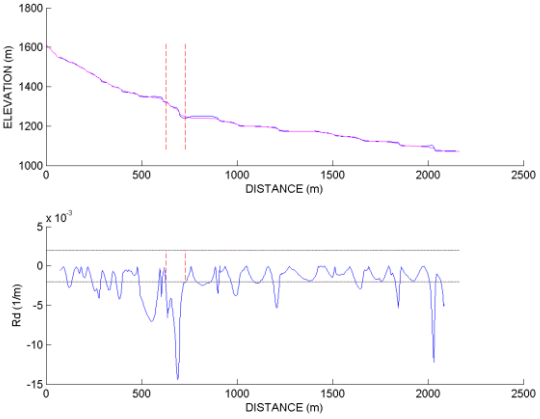

(a) Topographical nodes and R_d threshold

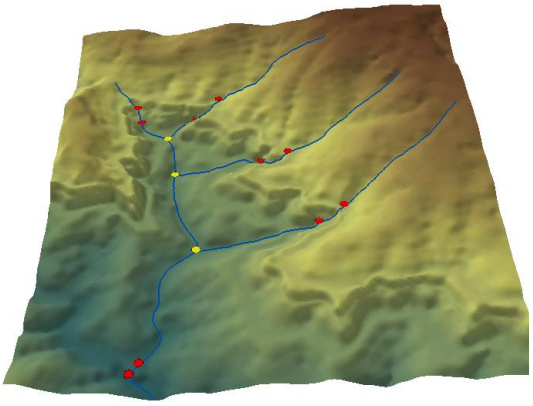

(b) DEM, drainage network and topographic nodes locations

Figure 5-4. Topographical nodes identification using the metric R_d

5.2.2 Channel Classification and Sizing

Once the drainage network is segmented, the defined reaches are characterized using the attributes illustrated in Figure 5-5. The reach slope S_0 is estimated as the ratio between the drop height Δz and the reach length L_R, where the latter is estimated based on the accumulated distance map obtained through the DEM pre-processing. On the other hand, using the set of (x, y) coordinates along the set of cells defining a reach path, the median radius of curvature R_m and the median wavelength L_m can be estimated following the methodology posed by *Jiménez et al.* [__] which is, in turn, supported on the method for deriving meander bend properties proposed by *Dodov and Foufoula-Georiou* [2004].

Based on the slope and watershed area draining the reach -*A*-, it is used the morphological classification scheme proposed by *Flores et al.* [2006] to assign to each reach any of the morphological types or classes *cascade*, *step-pool*, *plane bed* o *pool-riffle*. In Figure 5-6a is shown the proposed classification tree, where $S_0 A^{0.4}$ defines the specific power index introduced in the classification scheme to differentiate stream classes having similar ranges of slope.

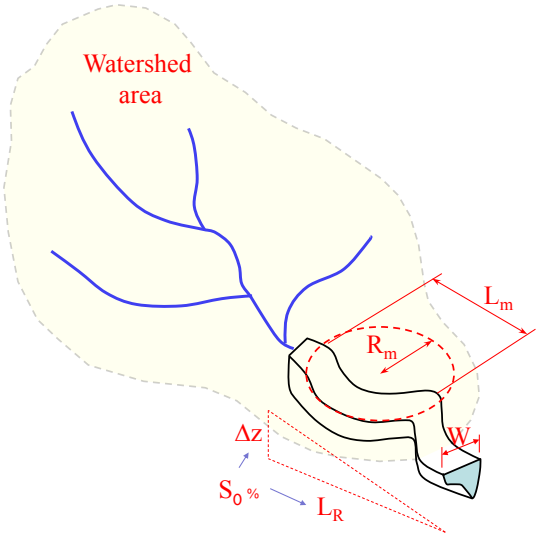

Figure 5-5. Schematic representation of the morphological features assessed in a reach

Cascade and *step-pool* are systems with high transport capacity, thus sediment yields are limited by the supply coming from upper areas. By contrast, *plane bed* and *pool-riffle* systems, are often limited not by sediment inflows but for their ability to transport it because of the low gradient they have.

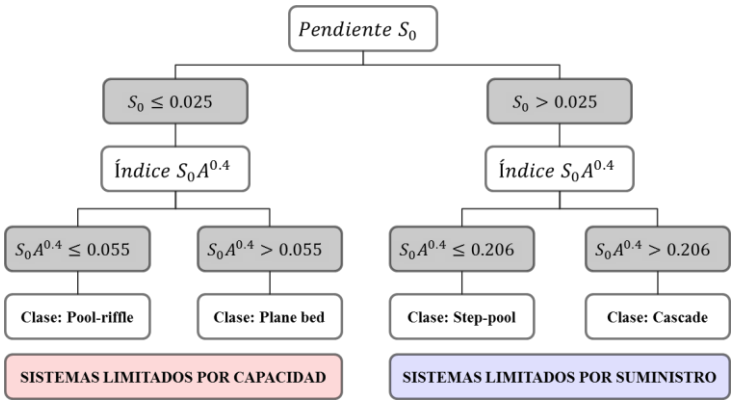

(a)

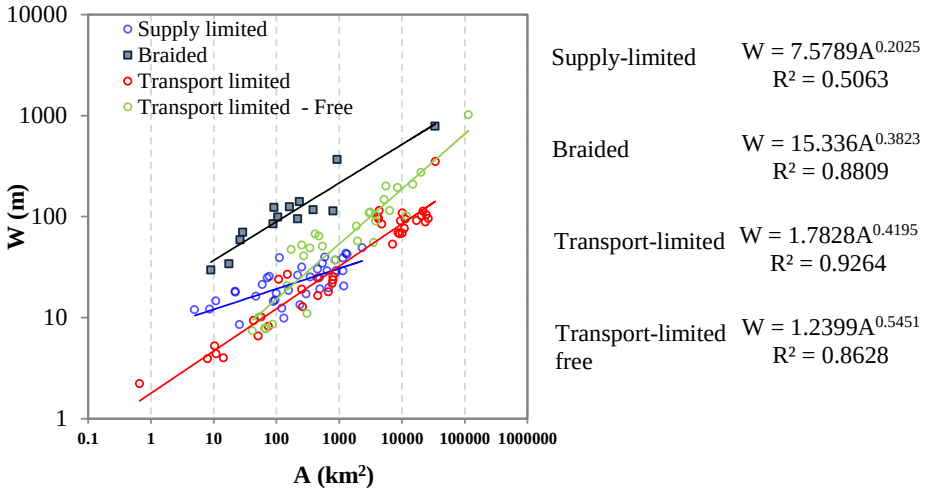

(b)

Figure 5-6. (a) Morphologic classification system by *Flores et al*. [2006] and (b) hydraulc geometry relations for bankfull width

Both categories were used in Chapter 4 to distinguish hydraulic geometry relations for bankfull width -W_B- as shown in Figure 5-6b, wherein it can noted the additional categories corresponding to braided and migrating (Free Transport-Limited) systems. Since such relations were derived using the watershed area as an independent variable, bankfull width W_B can be assessed for each stream reach. It should be noted that the attributes R_m y L_m are used to define reaches that can be considered as systems with low confinement, and therefore migrating.

5.2.3 Dispersion Mechanisms

The geometrical and morphological structure featuring a stream reach, determines how dissolved substances are transported downstream, since it has a direct influence on mechanisms such as differential advection and transient storage. At the reach scale, it has been shown that these processes can be aggregate into a lumped topological representation based on the Aggregated Dead Zone (ADZ) model. This kind of models are further especial at cases lacking detailed survey data regarding a stream geometry, which allow to set a hydraulic model wherein the velocity field can be represented by two-dimensional or three-dimensional schemes.

The ADZ model represents the complex geometric structure of a stream reach, through the topological representation shown in Figure 5-7. Surface and sub-surface areas favoring solute temporal retention are represented by the lumped dead zone element placed at the downstream edge.

A solute entering at the upstream edge with a concentration of $C_u(t)$ initially moves along a pure advective transport zone during the period τ, and then it enters to the active zone ADZ where longitudinal dispersion, transversal dispersion and temporal storage are represented. In this zone, the solute resides a period T_r, which relates to τ and the mean travel time along the entire reach t_m, according to equation (5-2). It must note that only a volume fraction DF (Dispersive Fraction) within the reach is considered as completely mixed, which can be estimated following equation (5-3).

$$t_m = \tau + T_r \quad 5\text{-}2$$

$$DF = 1 - \frac{\tau}{t_m} \quad 5\text{-}3$$

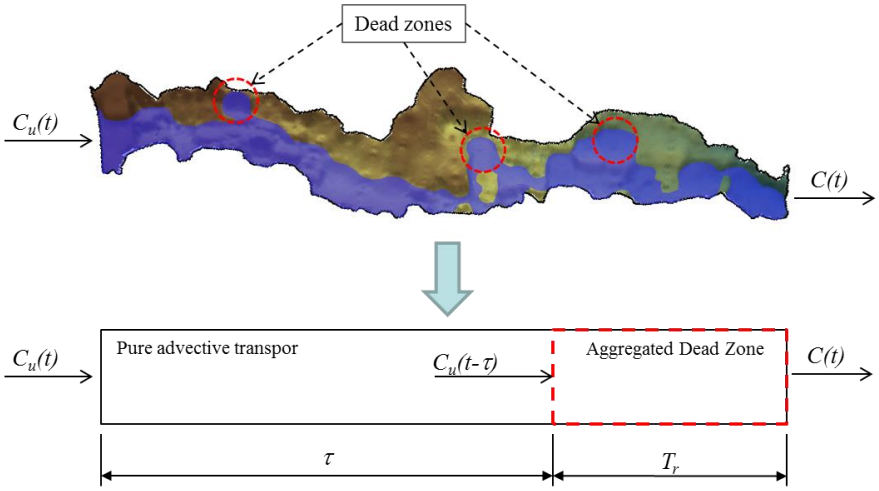

Figure 5-7. Topologic representation of a stream reach base on ADZ model

The concentration at the downstream edge $C(t)$, can be related to the input concentration and the time parameters t_m y τ according to equation (5-4) [*Lees et al.*, 2000].

$$\frac{dC(t)}{dt} = \frac{1}{t_m - \tau}[C_u(t-\tau) - C(t)] \quad 5\text{-}4$$

González [2008] analyzed the behavior of *DF* in mountain rivers, and found that it has high variability in contrast of lowland rivers, and suggests using a magnitude of $DF = 0.272 \pm 0.015$ when detailed information (tracer data, topographical surveys, etc.) is not available. *Jiménez and Wohl* [2013] also found a high *DF* variability in *step-pool* channels, and they also found that this

parameter as well as travel times t_m y τ, are closely related to morphological features of those morphologic systems.

Camacho and Lees [2000] posed a strategy to estimate the travel times t_m y τ through the ADZ-MDLC integrated solute and flow routing method. By this strategy, the ADZ parameters can be obtain by using reach-averaged hydraulic variables (top with, normal depth and mean flow velocity) and hydraulic parameters (Manning coefficient).

In the *Distributed Solute Transport Model* the contributions previously mentioned are integrated to characterize solute transport mechanisms in the drainage network. Figure 5-8 displays schematically the strategy for selecting the approach used to estimate the parameters t_m, τ or DF, according to the morphological class assigned to each stream reach in the segmentation procedure.

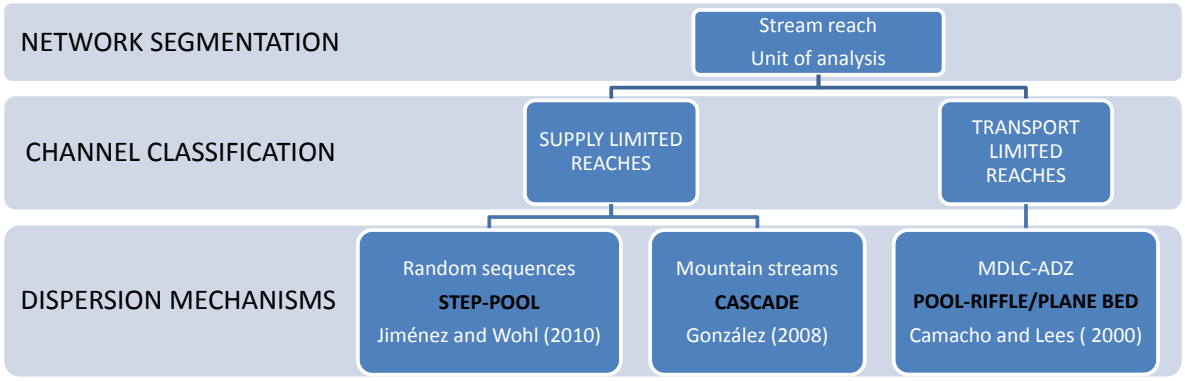

Figure 5-8. Strategy selection to parameterized the ADZ model according with a stream reach morphological class

5.2.4 Uncertainty Analysis

The proposed distributed model has different sources of uncertainty that can be taken into two different groups. The first refers to sources inherently related with DEMs, which are propagated due to the watershed area required to estimate both the bankfull width W_B, and the specific stream power index $S_0 A^{0.4}$ necessary, in turn, into the morphological classification scheme. Likewise, stream gradient S_0 is a sensitive variable to DEM resolution changes. The second group makes reference to contributions coming from the empirical relationships used for sizing reaches and those corresponding to parameterizations of the ADZ model. In this section, it is describe the way to consider the second type of contributions into de The *Distributed Solute Transport Model*.

For each simulation, watershed area and channel slope for a reach are fixed variables and therefore the corresponding morphological class (Steps 1 and 2 in Figure 5-9). According to the morphological class assigned, it is chosen the hydraulic geometry relation that better describes the bankfull width, as shown in Step 3. However, instead of using the estimated value with the relation $W_B - A$, a random number is generated within the interval $[W_B min - W_B max]$, whose limits are defined in terms of the prediction intervals of the empirical relations suggested by *Jiménez et al.* [__], which are shown in Figure 5-10a and Figure 5-10b for supply-limited and transport-limited systems, respectively.

In the fourth step, additional uncertainty is generated depending on how the times t_m and τ are calculated. For *step-pool* systems *Jiménez and Wohl* [2013] showed that the random arrangements of step-pool-run sequences are the main sources of uncertainty, followed by the estimation of the mean travel time using the dimensionless empirical relation $t_m^* - q^*$. Briefly, uncertainty propagation in high-gradient reaches is doing by both the generation of random sequences which, in turn, depend on the bankfull width, and the use of the prediction intervals for the $t_m^* - q^*$ relation.

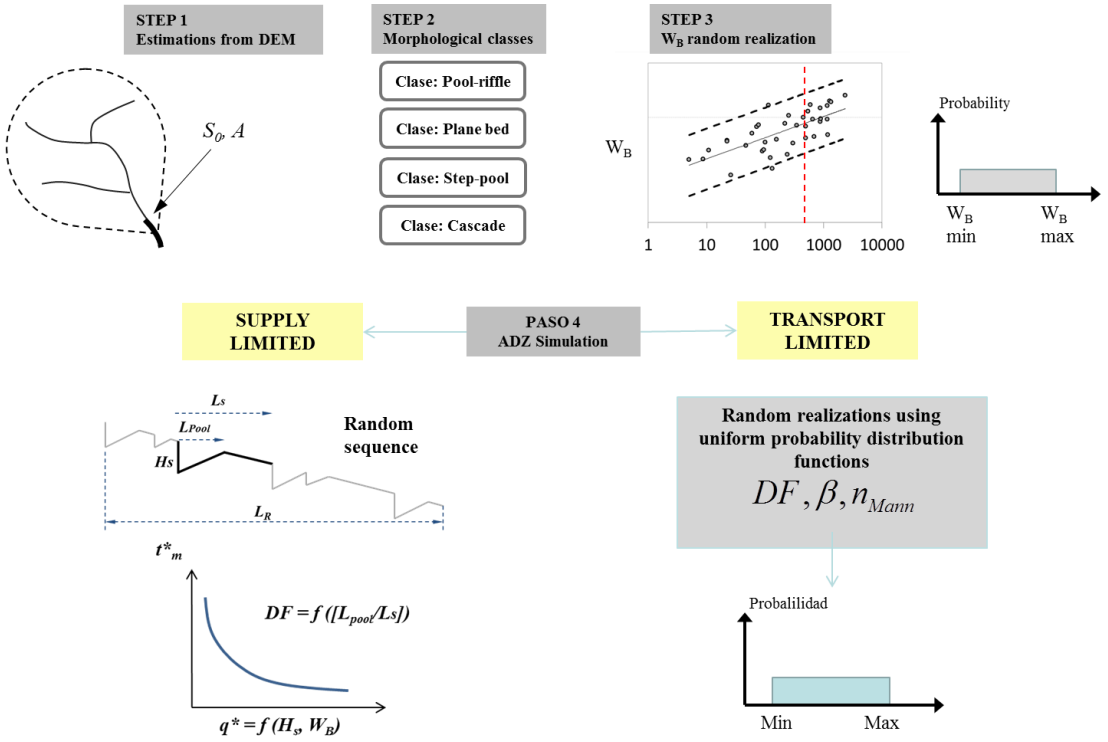

Figure 5-9. Uncertainty analysis assessment consider in the *Distributed Solute Transport Model*

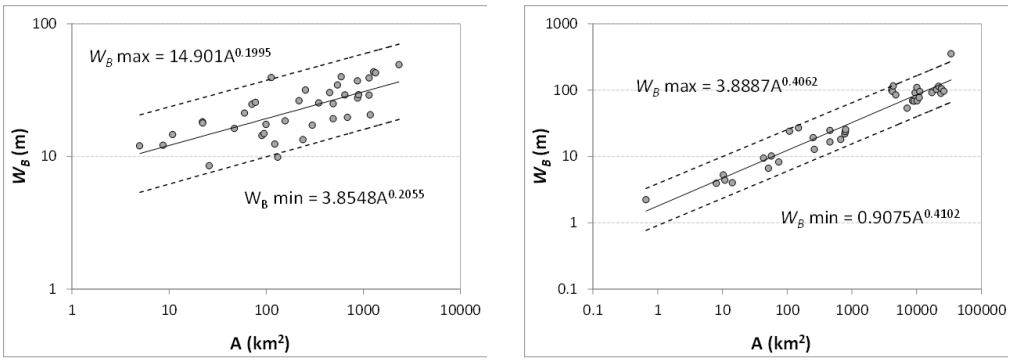

(a) Supply-limited (b) Transport-limited

Figure 5-10. Prediction intervals for the adopted hydraulic geometry equations of bankfull width

For transport-limited systems besides the bankfull width, the random set of parameters includes the dispersive fraction *DF* and the "*solute-lag*" coefficient β [*Camacho*, 2000], that relates the mean flow velocity with the average velocity of the solute. The variability of these parameters are set in the intervals [0.02 to 0.70] and [0 - 1.2] respectively, taking into account the objective calibration of the model MDLC-ADZ carried out in 70 reaches studied in the Bogotá river basin [*Universidad Nacional de Colombia – Empresa de Acueducto de Bogotá*, 2009].

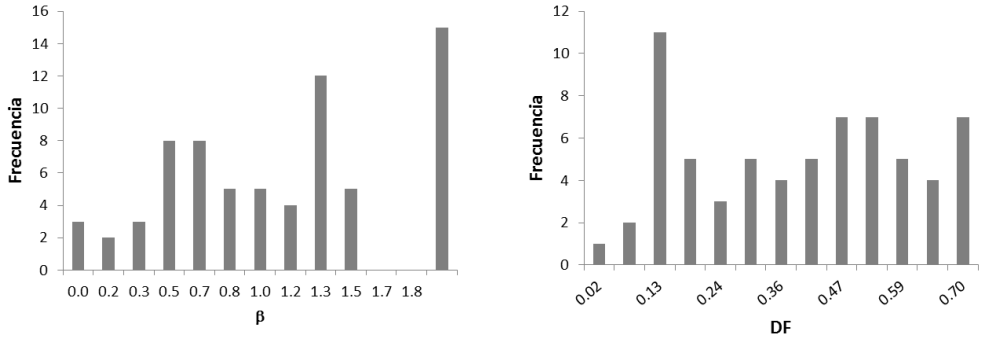

(c) "*solute-lag*" coefficient (d) Dispersive fraction

Figure 5-11. Variability of *DF* y β base on analyses carried out at 70 stream reached having slopes below than 2.5 % [*Universidad Nacional de Colombia – Empresa de Acueducto de Bogotá*, 2009]

5.3 MODEL IMPLEMENTATION AND VERIFICATION

In this section the model performance is evaluated using synthetic information in La Mosca watershed, which is located in the east of the department of Antioquia (Colombia), and has a catchment area around 155 km^2. La Mosca creek provides water supply for several purposes, but it is also used for residential and industrial wastewater disposal. One the major tributaries from the

west, La Brizuela creek, drains a catchment area of 7.1 km^2 and is characterize for having large gradients.

Figure 5-12 displays both watershed boundaries along which 10 control points (PC) have been placed in order to evaluate the influence of a synthetic solute spill defined at the upper part of La Brizuela creek. The solute spill has 1 m^3/s flow discharge and a concentration of 60 mg/L.

The test region features DEMs with resolutions of 90 m, 30 m and 10 m, associated to three different information sources. The first corresponds to the generated products by the Shuttle Radar Topographic Mission (SRTM), the second to the satellite mission ASTER (Advanced Spaceborne Thermal Emission and Reflection Radiometer) and the third, which was supplied by the local environmental center CORNARE, was used to define the topology of the drainage network by processing the DEM using a 1:25000 scale vector drainage network also provided by CORNARE.

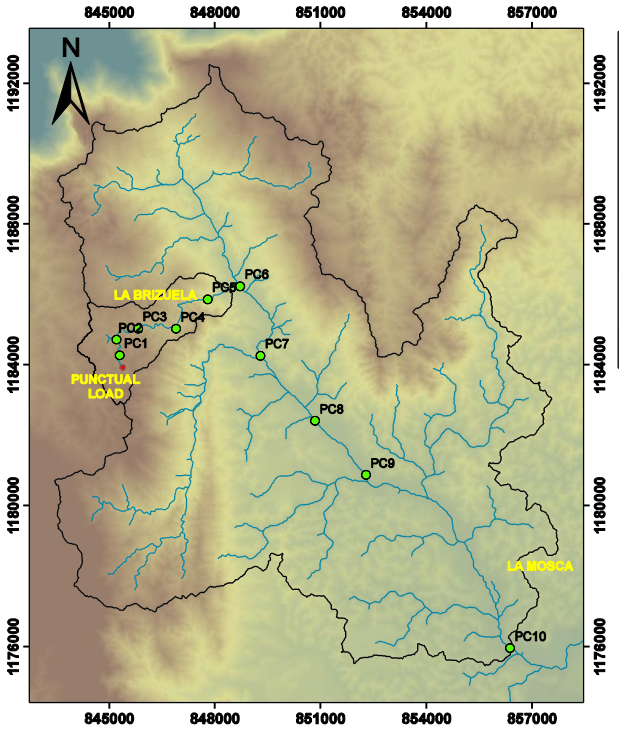

(a)

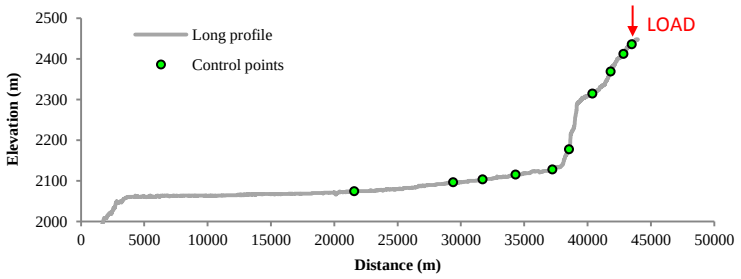

(b)

Figure 5-12. La Mosca y La Brizuela basins and location of the synthetic solute inyection and control points PC

For each case, a pre-processing was made using the MapWindow GIS to derive a flow direction map, a flow accumulation map (or catchment area), a cumulative distance map and the rasterized drainage network, all required as input data to implement the segmentation strategy, the morphological characterization and the downstream solute transport simulation along La Brizuela y La Mosca creeks. A mean flow map Q was estimated by a long-term water balance scenario described by equation (5-5), where P and E represent the mean precipitation and real evapotranspiration fields in the watershed [*CORNARE and UNALMED*, 2009], and A corresponds to the flow accumulated map.

$$Q = (P - E)A \qquad 5\text{-}5$$

Simulation was made for each resolution case using both a segmentation only based on hydrological nodes and including, additionally, topographical nodes as suggested in the methods here proposed.

5.3.1 Segmentation

After segmentation, it was found as the only sensitive parameter the window size N used for filtering and smoothing the longitudinal profile of streams. Figure 5-13a shows a longitudinal long profile extracted from the 90 m – resolution DEM, where the resulting topographical nodes are display as vertical dotted lines, which were obtained using a window size N = 10 cells. By using the same window size in the 30 m and 10 m resolution DEMs, it is clear in Figure 5-13b and Figure 5-13d that the method overestimates the number of topographic nodes required to represent adequately the longitudinal profile.

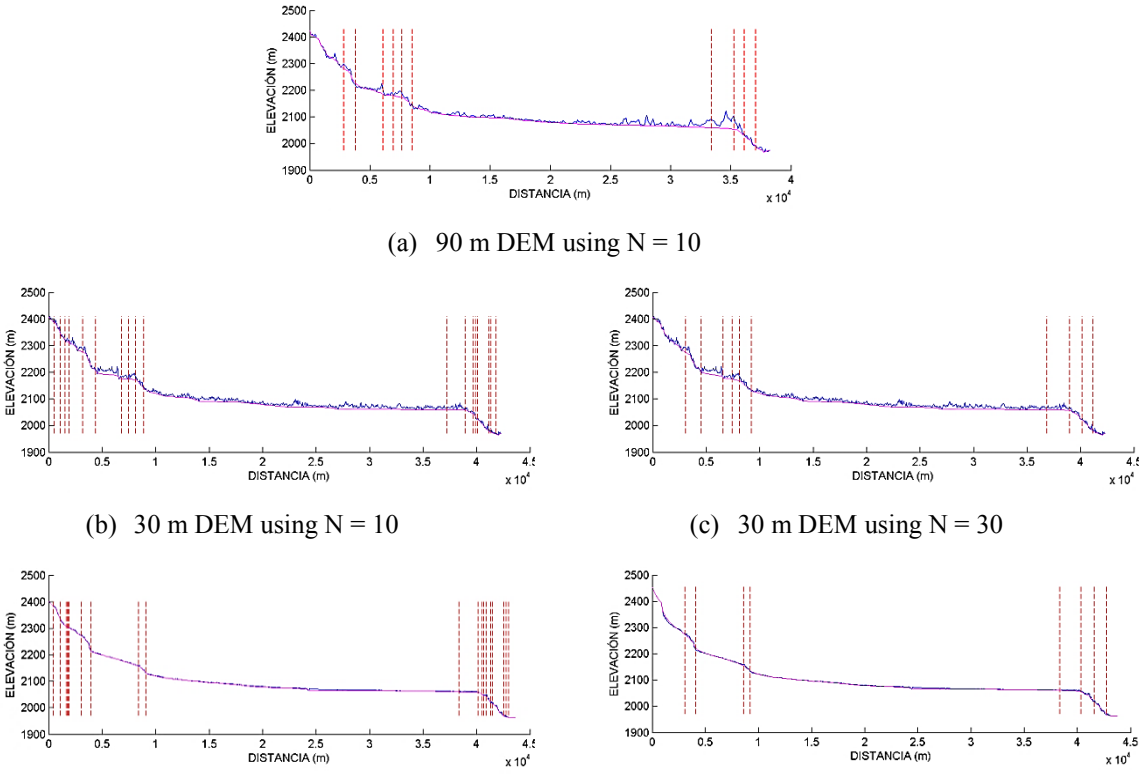

(a) 90 m DEM using N = 10

(b) 30 m DEM using N = 10

(c) 30 m DEM using N = 30

(d) 10 m DEM using N = 10

(e) 10 m DEM using N = 90

Figure 5-13. Evaluation of consistency of the model to identify topographical nodes using different DEM resolutions

However, when the parameter N is perturbed independently for each DEM it is possible to reach the same consistency level as shown in Figure 5-13c and Figure 5-13e. It also worth noticing that the finer resolution the higher window size required. Nonetheless, more than establishing a resampling rule it is considered that each region should be analyzed independently since topographic break on slopes not necessarily obey the same physical forcing factors characterizing La Mosca watershed.

Using cells of 10, 30 and 90 for the DEMs of 90 m, 30 m and 10 m, respectively, is obtained the spatial distribution of hydrological and topographic nodes shown in Figure 5-14, which are also displayed downstream along the main longitudinal profiles. It should be noted that even though the noise in the longitudinal profiles is higher as DEM resolution get lower, the smoothing and filtering methods carried out prior to the identification of topographic nodes lead to more consistent results.

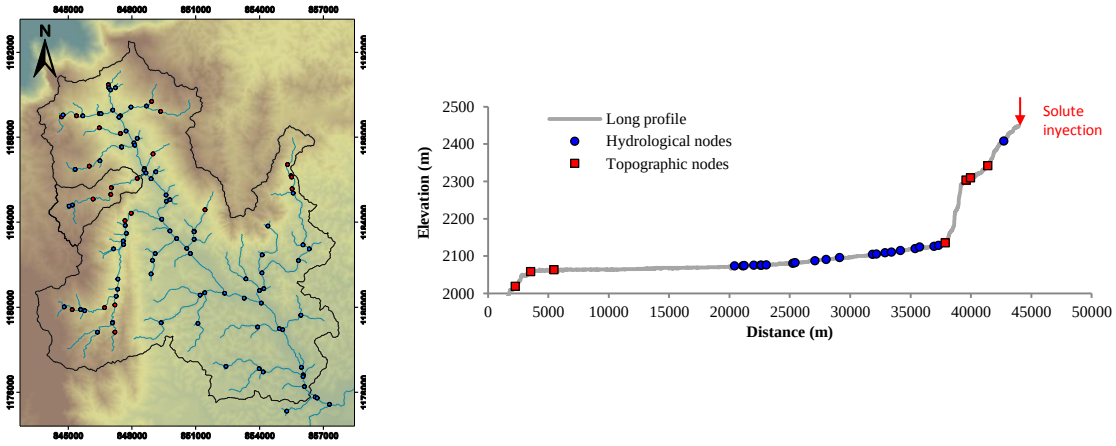

(a) 10 m DEM

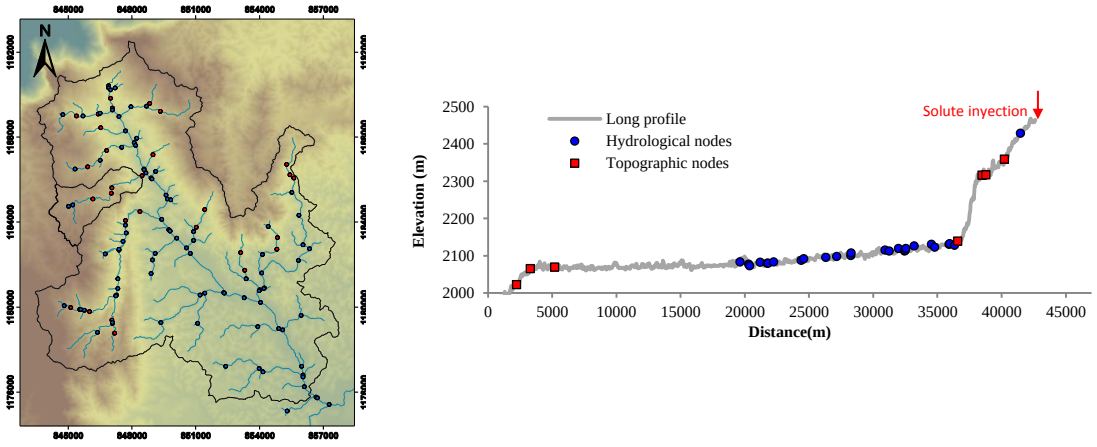

(b) 30 m DEM

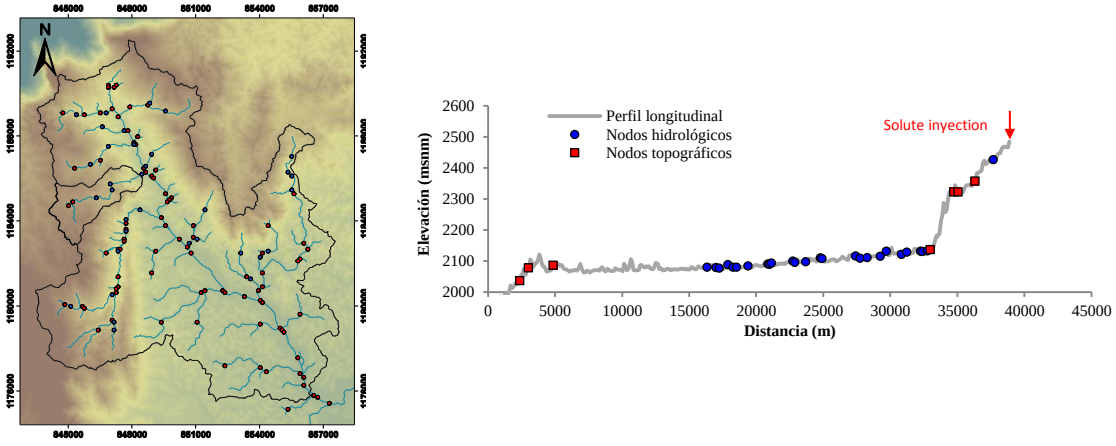

(c) 90 m DEM

Figure 5-14. Nodes definition in La Mosca basin for different DEM resolutions

5.3.2 Solute transport

A total reach number of 197, 218 and 221 are obtained for DEM resolutions of 10 m, 30 m and 90 m, respectively. The slope-area diagram for each case is presented in Figure 5-15, where the general trend of data suggests both, a decreasing in slope S_0 as DEM resolution becomes finer, and higher dispersion of the results taking into account declination of the determination coefficient R^2. Unlike, slope gradient do not have any systematic variation with resolution changes along the analyzed stream corridor, as seen in Figure 5-15d, except by the high differences always persisting in the upper part of the watershed (between PC1 and PC6). On the other hand, Figure 5-15e suggests that differences in slope gradient are more related to the elevation values sampled from each DEM than in the river lengths which showed no significant variability at resolution changes (Figure 5-15e).

Among the implications of the latter is the difference in the spatial distribution of morphological types along the longitudinal profile, obtained for each resolution case after using the morphological classification scheme by *Flores et al.* [2006]. Stream-reach types are shown in Figure 5-16a to Figure 5-16c, where differences can be seen upper areas in La Brizuela as well as in some the reaches located downstream the confluence on La Mosca creek.

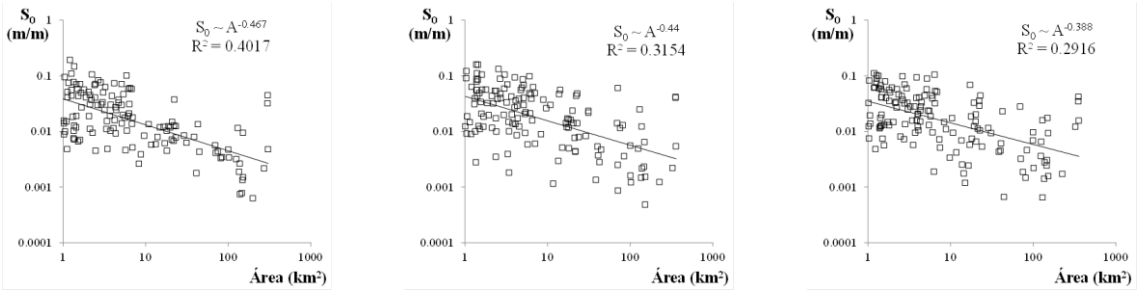

(a) 10 m DEM (b) 30 m DEM (c) 90 m DEM

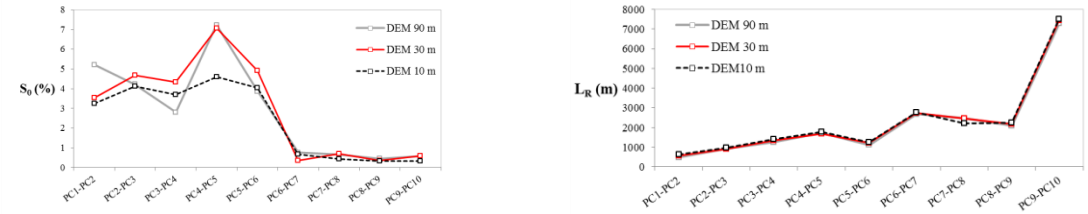

(d) Slope changes (e) River legth changes

Figure 5-15. Slope-area diagram changes with DEM resolution, and slope and river length sensivity

Based on the morphological classification made in each case, it was adopted the parameters of the transport model ADZ according to the diagram shown in Figure 5-8. In this way, travel times t_m and τ are estimated for all reaches and their corresponding stream flow according to the map Q.

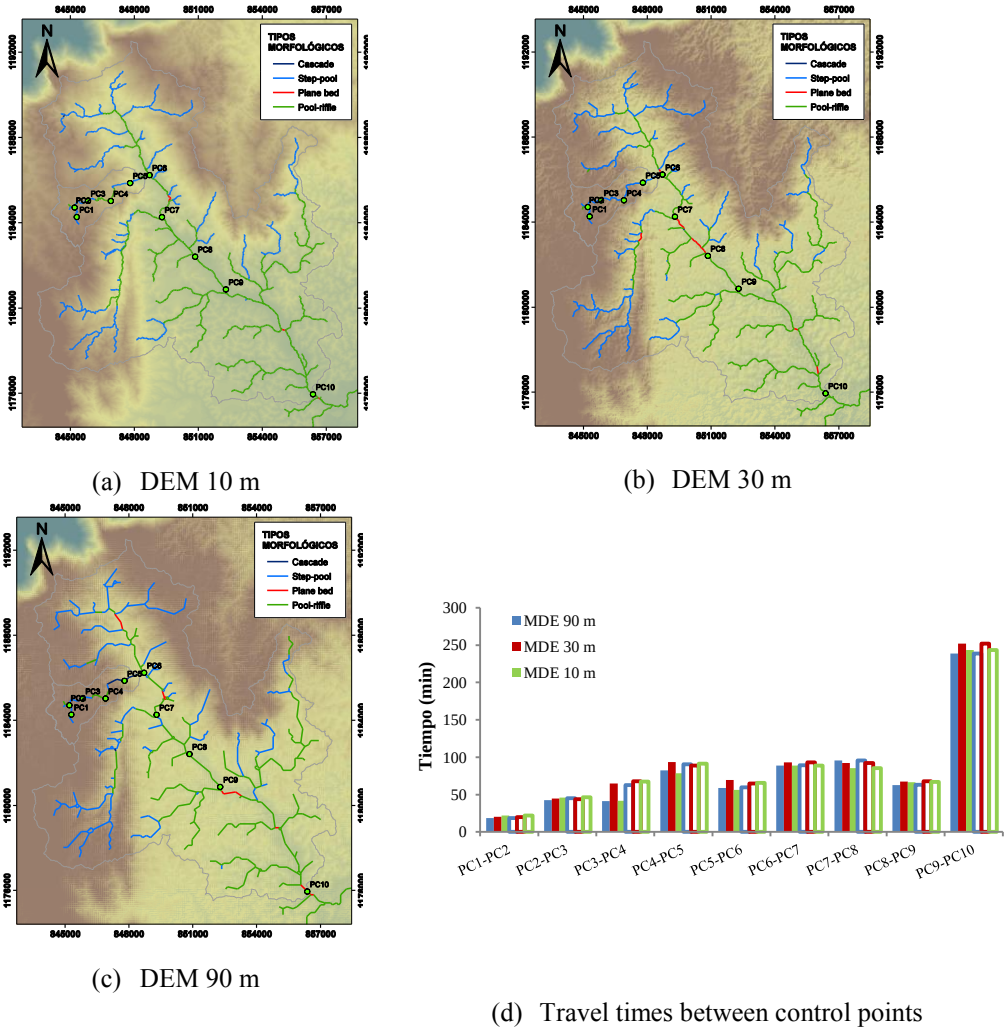

(a) DEM 10 m

(b) DEM 30 m

(c) DEM 90 m

(d) Travel times between control points

Figure 5-16. Stream classification and DEM resolution, and comparisons between travel time estimation using the proposed segmentation and the separation of reaches only based on hydrological nodes

Given the uncertainty propagation that naturally occurs downstream in the simulation process, comparisons where made not only at the outlet of the basin (PC10), but also between consecutive control points as shown in Figure 5-16d, using as reference values the travel times obtained from the highest resolution DEM (10 m). Solid bars correspond to outcomes obtained using a network segmentation based on hydrological and topographic nodes, whilst the values represented by unfilled bars were obtained considering only hydrological nodes.

The simulated breakthrough curves for some control points are displayed in Figure 5-17, where concentrations were normalized to allow making comparisons. Results show correspondence between the results obtained from the 10 m and 90 m DEMs. However, the obtained signal at PC4 site using the 30 m DEM has is delayed about 23 min, thus influencing the remaining signals downstream. A closer inspection of the segment PC3-PC4 reveals that this is set by two reaches regardless of DEM resolution as shown in Table 4-1, however, the second reach was defined as a *step-pool* channel for the 30 m DEM, in contrast to the *pool-riffle* system obtained by using the other resolutions. It should be noted that as a consequence of the simulation framework, the mentioned differences lead to both, differences in the hydraulic geometry relation used to estimate the bankfull width W_B, and differences in the ADZ model parameterization, which together and naturally leads to deviations between the simulated time-concentration curves.

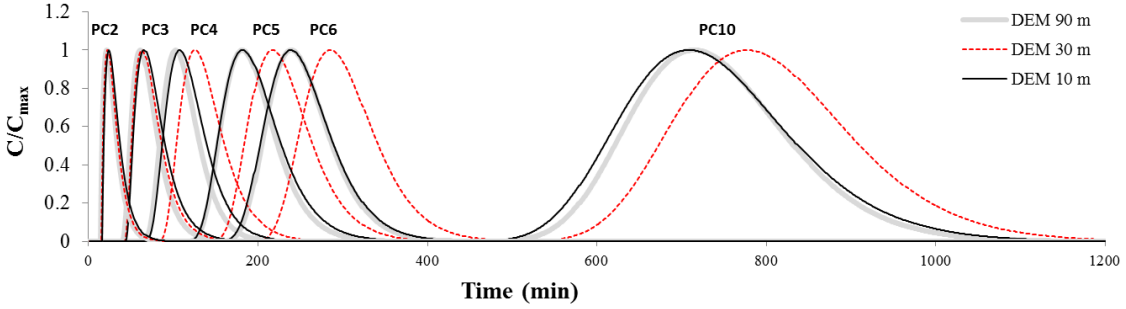

Figure 5-17. Diagramas tiempo-concentración simulados hacia aguas abajo en sitios de control para las diferentes resoluciones del MDE de la zona de estudio

Table 4-1. Morphologic features of segment PC3-PC4

DEM resolution	Segment label	Reach code	L_R (m)	Segment length (m)	S_0 (%)	Morphologic type
10 m	PC3-PC4	201	394	1394	4.9	Step-pool
		125	1000		2.4	Pool-riffle
30 m	PC3-PC4	222	375	1351	5.8	Step-pool
		135	976		2.8	**Step-pool**
90 m	PC3-PC4	225	558	1258	3.2	Step-pool
		137	700		2.3	Pool-riffle

Comparisons among travel times (t_m) between control points, show that deviations between the 90 m DEM and the 10 m DEM do not exceed the 15.1% (Table 4-2). By contrasts and as it was expected, the largest deviations corresponds to the 30 m DEM, which in turn are attenuated as the solute is transported downstream.

Table 4-2. Relative differences between temporal parameters between control points. Topographical and hydrological nodes were used to separate stream reaches. Reference values correspond to those obtained using the 10 m DEM

Tramo	Mean travel time t_m			Time delay τ		
	DEM 90 m	DEM 30 m	DEM 10 m	DEM 90 m	DEM 30 m	DEM 10 m
PC1-PC2	-15.1	-8.1	***	-15.4	-7.7	***
PC2-PC3	-7.6	-2.4	***	-6.9	0.0	***
PC3-PC4[1]	-0.3	55.4	***	3.8	65.4	***
PC4-PC5[2]	4.8	18.9	***	7.3	25.5	***
PC5-PC6[3]	4.6	24.1	***	4.7	23.3	***
PC6-PC7	0.4	5.0	***	3.5	8.8	***
PC7-PC8	12.2	8.3	***	11.9	11.9	***
PC8-PC9	-6.0	0.9	***	-5.6	2.8	***
PC9-PC10	-1.9	3.5	***	4.0	4.0	***

[1,2,3] Highest relative deviations

A similar analysis was made but this time by making comparisons between the travel time presented in Table 4-2, with those obtained using only hydrological nodes into the segmentation procedures. It can be noticed in Table 4-3 that the higher deviations correspond to the finer and coarser DEMs, with the highest at the PC3-PC4 segment which was classified as *pool-riffle* according with Table 4-1. Hence, the overestimation of t_m appears, again, as a consequence of the *step-pool* stream type assigned when it is only consider hydrological nodes.

Table 4-3. Relative differences between temporal parameters between control point. Network segmentation is only based on hydrologic nodes. Reference values correspond to those obtained using the segmentation procedure proposed in this study.

Tramo	Tiempo medio t_m			Tiempo primer arribo τ		
	DEM 90 m	DEM 30 m	DEM 10 m	DEM 90 m	DEM 30 m	DEM 10 m
PC1-PC2	0.0	-1.2	1.4	0.0	0.0	0.0
PC2-PC3	6.7	-1.6	0.9	7.4	-3.4	0.0
PC3-PC4[1]	51.3	4.8	61.5	44.4	-4.7	61.5
PC4-PC5[2]	10.0	-5.0	16.6	-1.7	-17.4	7.3
PC5-PC6	2.1	-7.0	17.5	-4.4	-11.3	9.3
PC6-PC7	0.3	0.2	0.2	1.7	-3.2	1.8
PC7-PC8	-0.1	0.1	0.0	1.3	1.3	1.5
PC8-PC9	0.5	0.4	0.5	2.9	0.0	2.8
PC9-PC10	0.0	0.0	0.0	1.7	1.1	2.3

[1,2] Mayores desviaciones porcentuales absolutas obtenidas

5.4 DISCUSSION AND CONCLUSION

A method to separate and to morphologically characterize stream reaches was tested using digital elevations models (DEMs) available in La Mosca watershed, with coherent results.

However, slope gradient appeared to be a high sensitive variable due to the inherent sampling and averaging techniques depending on which DEM is used. This statement is also supported by the fact that river lengths did not suffer significant changes when DEM resolution was changed.

Despite the latter do not have implications in the identification of hydrological and topographic nodes and on the subsequent drainage network segmentation, a misleading morphological classification was identify at the upper part of the analyzed longitudinal profile for the 30 m DEM. This issue, at the same time, had a direct influence on the ADZ model parameterization to determine t_m and τ. Given such limitation, further analysis should be carried out in order to understand not only how slope gradient is locally (at the reach-scale) affected when a DEM is resampled or when different data sources are used, and to propose a strategy which allows minimizing those changes. Additionally, a more detailed analysis can be carrying out to determine objectively the window size N required into the smoothing and filtering methods used by the *Distributed Solute Transport Model*. Alternatively, a multi-resolution analysis can be used to cross-validate different DEMs, taking into account the study area extension and the computational cost when implementing the *Distributed Solute Transport Model*.

It worth underscores that dispersion assessment in the model, is underlain by the morphological classification scheme proposed by *Flores et al.* [2006], which is limited to four alluvial morphological classes with a single thread or main channel. In this regard, the *Distributed Solute Transport Model* is susceptible to be extended to consider more robust morphological classification scheme, which account for lateral confinement degree and metrics to identify multiple thread systems (braided channels). For the first case, the ratio between the median wavelength and the mean bankfull width can be used to distinguish migrating systems from those with some level of confinement, either by lithology factors or related to riparian vegetation along the stream corridor. However, assessment of metrics to describe stream patterns requires DEM resolutions comparable with the channel size in order to have representative values. More complex is the case for braiding systems, which despite of having a clear hydraulic geometry relation for bankfull width, they cannot be identified based only on slope gradient and watershed area. It requires additional information which allows to compare the supply of sediment with the transport capacity of the reach [*Leopold and Wolman*, 1975; *Kellerhals and Churc*, 1989; *Beechie et al.*, 2006].

Additional limitations of the model were addressed through Monte Carlo simulations considering the uncertainty sources related to the adopted empirical schemes. Following the

uncertainty analysis scheme described in section 5.2.4 (using 200 Monte Carlo simulations), are obtained the time-concentration diagrams shown in Figure 5-18 for the PC2, PC6 and PC10. The shaded area is defined by the 5% and 95% and the 50% quantile is given by the blue line. It should be noted that the simulated concentrations were normalized to the maximum concentration of 50% quantile.

The results suggest that the uncertainty in the estimation of the peak concentration decreases downstream, unlike the uncertainty in the estimation of arrival times of the solute.

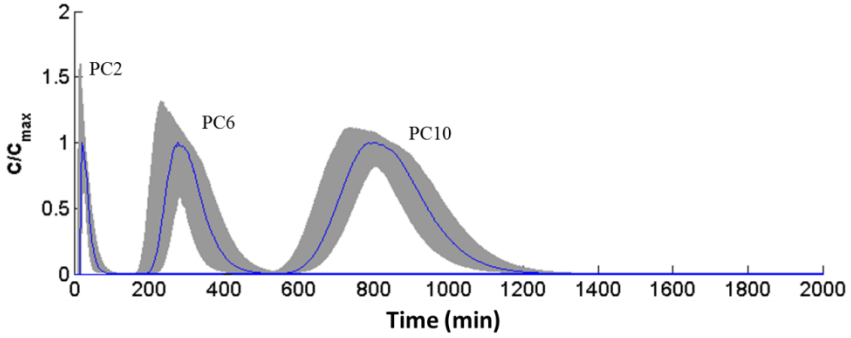

Figure 5-18. Uncertainty propagation downstream

For a continuous solute injection and steady flow conditions, the simulation scheme does not suggests uncertainty due the complete mixing occurring in the drainage network, as shown in the concentration profile illustrated in Figure 5-19a. For such condition, the uncertainty generated by the model becomes relevant when the solute is likely to transform its nature as it is transported downstream, an aspect of particular interest in the simulation of surface water quality and wherein the *Distributed Solute Transport Model* can be used as a support tool in the management of water resources.

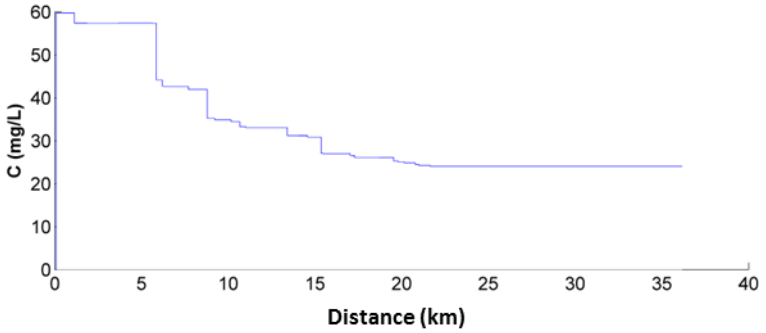

(a)

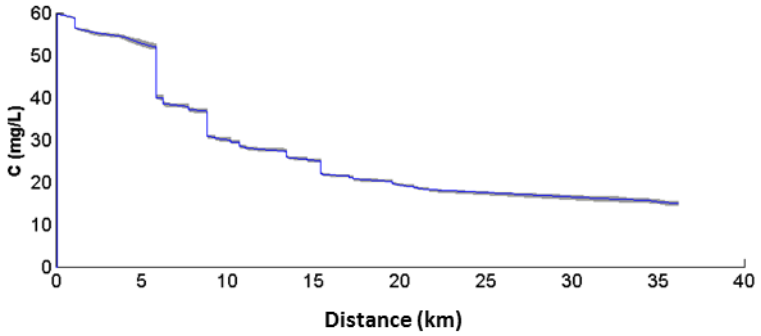

(b)

Figure 5-19. Concentration profiles for a conservative (a) and a non-conservative (b) solute, continuously injected upstream

5.5 ACKNOWLEDGEMENTS

Thanks to COLCIENCIAS and Universidad Nacional de Colombia for funding the PhD studies of the first author through the project *Integrated Management of Joint Use of Superficial and Ground Water*. In the same way, thanks also to CORNARE which was always open to supply map data of their jurisdiction.